966 *Chem. Mater.* **2010,** *22,* 966–973
DOI:10.1021/cm901855y

CHEMISTRY OF MATERIALS
Article

Synthesis and Characterization of Three-Dimensionally Ordered Macroporous (3DOM) Tungsten Carbide: Application to Direct Methanol Fuel Cells†

Jeffrey P. Bosco,‡ Keisuke Sasaki,§ Masahiro Sadakane,⊥ Wataru Ueda,§ and Jingguang G. Chen*,‡

‡*Department of Chemical Engineering, University of Delaware, Newark, Delaware 19716,* §*Catalysis Research Center, Hokkaido University, N-21, W-10, Sapporo 001-0021, Japan, and* ⊥*Chemistry and Chemical Engineering, Graduate School of Engineering, Hiroshima University, 1-4-1 Kagamiyama, Higashi-Hiroshima 739-8527, Japan*

Received June 29, 2009. Revised Manuscript Received August 19, 2009

Three-dimensionally ordered macroporous tungsten carbide (3DOM WC) with varying pore size was synthesized using the "inverse-opal" method. Poly{methyl methacrylate} (PMMA) colloidal crystal template with sphere diameters ranging from 180 to 490 nm was used. Two synthesis procedures were performed, the first requiring calcination of tungsten impregnated PMMA colloidal template in air followed by carburization in $H_2/CH_4/N_2$ atmosphere. The second procedure involved direct carburization of the tungsten impregnated template without prior calcination. The effect of Pt-modification of the template prior to carburization on the resulting material composition was also investigated. The material properties were evaluated using surface and bulk characterization techniques. Finally, cyclic voltammetry was used to investigate the methanol electro-oxidation activity of the 3DOM WC and Pt-modified 3DOM WC in acidic electrochemical environment.

1. Introduction

The search for a low-cost, high-activity anode electrocatalyst for application in direct methanol fuel cells (DMFC) is of growing interest as demand continues to rise for portable, high energy-density power sources. The current catalysts used in DMFC applications rely primarily on supported Pt and Pt−Ru bimetallic catalysts. In addition to their high cost, Pt and Pt−Ru catalysts are prone to CO-poisoning at active sites, substantially decreasing their potential for use in devices employing alcohols or low-purity H_2 as the fuel source.[1−3] Investigations in this area have uncovered a number of potential materials that are more CO-tolerant at PEM fuel cell temperatures, including transition metal carbides and oxides materials. In particular, tungsten monocarbide (WC) materials have demonstrated Pt-like surface properties in many surface science and catalysis studies, including those first performed by Levy and Boudart and more recently by Chen et al.[4−9]

Investigations performed by Chen et al. demonstrated the stability and enhanced CO tolerance of WC under both ultrahigh vacuum and electrochemical environments.[6−9] Studies have also shown that C/W(110) and C/W(111) single crystal surfaces are more active than Pt(111) and Ru(0001) toward the dissociation of water and decomposition of methanol at low temperatures.[5,10] Additionally, when C/W surfaces were modified with submonolayer coverage of Pt metal, the electrochemical stability of WC is further increased.[8,9]

One major obstacle involved with the implementation of WC as a DMFC catalyst is the difficulty in obtaining a material with sufficiently high specific surface area while maintaining the desired stoichiometry (W:C = 1:1) and surface composition. Typical WC surface areas fall in the range of 1−35 $m^2\ g^{-1}$.[11−14] There are also studies that have reported WC materials with specific

† Accepted as part of the 2010 "Materials Chemistry of Energy Conversion Special Issue".

*Corresponding author. E-mail: jgchen@udel.edu. Fax: (302) 831-1048.

(1) Waszczuk, P.; Wieckowski, A.; Zelenay, P.; Gottesfeld, S.; Coutanceau, C.; Leger, J. M.; Lamy, C. *J. Electroanal. Chem.* **2001**, *511*, 55.
(2) Seiler, T.; Savinova, E. R.; Friedrich, K. A.; Stimming, U. *Electrochim. Acta* **2004**, *49*, 3927.
(3) Mavrikakis, M.; Greeley, J. *J. Am. Chem. Soc.* **2002**, *124*, 7193.
(4) Levy, R. B.; Boudart, M. *Science* **1973**, *181*, 547.
(5) Hwu, H. H.; Chen, J. G.; Kourtakis, K.; Lavin, J. G. *J. Phys. Chem. B* **2001**, *105*, 10037.
(6) Zellner, M. B.; Chen, J. G. *Catal. Today* **2005**, *99*, 299.
(7) Mellinger, Z. J.; Weigert, E. C.; Stottlemeyer, A. L.; Chen, J. G. *Electrochem. Solid-State Lett.* **2008**, *11*, B63.
(8) Weigert, E. C.; Stottlemyer, A. L.; Zellner, M. B.; Chen, J. G. *J. Phys. Chem. C* **2007**, *111*, 14617.
(9) Weigert, E. C.; Zellner, M. B.; Stottlemeyer, A. L.; Chen, J. G. *Top. Catal.* **2007**, 46.
(10) Zellner, M. B.; Chen, J. G. *J. Electrochem. Soc.* **2005**, *152*, A1483.
(11) Leclercq, G.; Kamal, K.; Lamonier, J. F.; Feigenbaum, L.; Malfoy, P.; Leclercq, L. *Appl. Catal., A* **1995**, *121*, 169.
(12) Ma, C.; Sheng, J.; Brandon, N.; Zhang, C.; Li, G. *Int. J. Hydrogen Energy* **2007**, *32*, 2824.
(13) Medeiros, F. F. P.; da Silva, A. G. P.; de Souza, C. P.; Gomes, U. U. *Int. J. Refract. Met. Hard Mater.* **2009**, *27*, 43.
(14) Giraudon, J. M.; Devassine, P.; Lamonier, J. F.; Delannoy, L.; Leclercq, L.; Leclercq, G. *J. Solid State Chem.* **2000**, *154*, 412.

 Published on Web 09/16/2009

surface areas approaching or greater than 100 $m^2\ g^{-1}$.[15] However, there is some question as to whether these high surface areas are due to the presence of surface carbon on the WC material. The current study demonstrates the susceptibility of WC synthesis to surface carbon impurities that may not be immediately detected through standard characterization techniques.

Because it may not be possible to obtain a WC material of the necessary high surface area due to the relatively high density of the material and high temperatures at which carbide synthesis is performed (therefore favoring crystallite sintering), it is important to achieve effective utilization of the available catalytic surface. Ordered microporous and macroporous materials demonstrated enhanced mass transport properties over those without porous structure in many gas and liquid phase applications.[16−18] The microchannels present in three-dimensionally ordered macroporous (3DOM) structures are particularly useful for catalysis applications where it is advantageous to have low mass-transfer resistance between diffusing chemical species and the catalytic surface. Furthermore, the 3DOM structure provides an ideal support for Pt-modification of WC, without requiring the addition of noncatalytic support materials. Stein et al. recently produced inverse-opal tungsten carbide with pore spacing of approximately 250 nm using WCl_6 and PMMA colloidal crystal template.[19] Although they did not produce tungsten carbide with the desired stoichiometry, their results demonstrated the feasibility of synthesizing this type of material with conventional carburization procedures.

The objective of the present work is to demonstrate the feasibility of synthesizing phase pure (W:C = 1:1) 3DOM tungsten carbide of adjustable pore size and its application as a potential electrocatalyst in DMFC. Differing from previous studies, ammonium metatungstate (AMT) was employed as a stable and inexpensive tungsten precursor and alternative to WCl_6. PMMA crystal templates with particle diameters ranging from 180 to 490 nm were also employed. Two carburization procedures adopted from previous studies were used for the synthesis.[19] The first produced 3DOM tungsten oxide (WO_3) by calcination of tungsten impregnated PMMA template followed by carburization to WC. The second method involved directly carburizing impregnated PMMA template without prior calcination. The heating rates and synthesis gas mixture used for these procedures were optimized in order to maximize the surface area of the resulting 3DOM materials by minimizing WC crystallite size while still maintaining the desired stoichiometric composition and structural stability. Finally, the effect of Pt modification of the template prior to carburization was investigated. The structure and composition of materials resulting from the two synthesis procedures were characterized using a wide range of surface and bulk characterization techniques. Finally, the electro-oxidation of methanol over 3DOM WC and Pt-modified 3DOM WC was evaluated under acidic environment using cyclic voltammetry. These studies were compared against Pt supported on carbon as a standard reference.

2. Experimental Section

2.1. Materials. All chemicals were reagent grade and used as purchased. Saturated aqueous ammonium metatungstate (AMT) solution (Nippon Inorganic Color & Chemical Co.; MW-2, 50 wt % as WO_3) was used as the W precursor and nitric acid solution with 4.557 wt % Pt metal (Tanaka Kikinzoku Kogyo) was used as a Pt precursor for all synthesis procedures. Methyl methacrylate monomer (Wako Pure Chemical Industries) and potassium peroxosulfate polymerization initiator (Katayama Chemical., LTD) were used for the synthesis of colloidal PMMA spheres. For cyclic voltammetry measurements of methanol electro-oxidation, pure methanol (99.5 wt %, Wako Pure Chemical Industries), sulfuric acid (98.5 wt %, Wako Pure Chemical Industries), and deionized water were employed.

2.2. Synthesis of 3DOM Tungsten Carbide. Suspensions of monodisperse poly{methyl methacrylate} (PMMA) spheres (diameters of 183 ± 6, 268 ± 9, 370 ± 8, and 490 ± 13 nm) were produced using standard techniques and packed into colloidal crystals with centrifuge.[20−22] The solid template was then crushed through testing sieves (Tokyo Screen, Co. LTD) to obtain uniform particle sizes between 0.425 and 2.000 mm. Crushed PMMA template (10 g) was immersed in tungsten solution (20 mL AMT solution, 10 mL MeOH) for a period of 3 h. The mixture was then filtered using a Buchner funnel for 30 min and the obtained solid was air-dried for several days resulting in W-impregnated PMMA template. For coimpregnation of Pt and W metals, PMMA template (5.0 g) was immersed in mixture of AMT solution (10 mL), MeOH (10 mL), and Pt solution (several grams). The mass of Pt solution added was varied depending on desired composition of WC material after carburization (1.8, 5.6, and 9.8 g of Pt solution for 1, 3, and 5 wt % Pt-WC, respectively).

For the synthesis of 3DOM WO_3, W-impregnated PMMA template (1.0 g) was mixed with quartz sand (5 g, 10−15 mesh, Kokusan Chemical Works). The mixture was calcined in a quartz-tube furnace at 500 °C (heating rate of 1 °C/min) for 5 h under flowing air (50 sccm). After calcination, the 3DOM WO_3 material was carefully separated from the quartz sand using a 0.425 mm sieve.

Identical carburization conditions were used for the indirect carburization of 3DOM WO_3 and direct carburization of W-impregnated PMMA crystal template to 3DOM WC. Carburization conditions were modified from previous procedures used for the standard WC synthesis.[23,24] Samples were placed in

(15) Ganesan, R.; Ham, D. J.; Lee, J. S. *Electrochem. Commun.* **2007**, *9*, 2576.
(16) Chai, G. S.; Shin, I. S.; Yu, J. S. *Adv. Mater.* **2004**, *16*, 2057.
(17) Liang, H.; Zhang, Y.; Liu, Y. *J. Nat. Gas Chem.* **2008**, *17*, 403.
(18) Munakata, H.; Yamamoto, D.; Kanamura, K. *J. Power Sources* **2008**, *178*, 596.
(19) Lytle, J. C.; Denny, N. R.; Turgeon, R. T.; Stein, A. *Adv. Mater.* **2007**, *19*, 3682.
(20) Sadakane, M.; Takahashi, C.; Kato, N.; Ogihara, H.; Nodasaka, Y.; Doi, Y.; Hinatsu, Y.; Ueda, W. *Bull. Chem. Soc. Jpn.* **2007**, *80*, 677.
(21) Zou, D.; Ma, S.; Guan, R.; Park, M.; Sun, L.; Aklonis, J. J.; Salovey, R. *J. Polym. Sci., Part A: Polym. Chem.* **2003**, *30*, 137.
(22) Lytle, J. C.; Yan, H.; Ergang, N. S.; Smyrl, W. H.; Stein, A. *J. Mater. Chem.* **2004**, *14*, 1616.
(23) Weigert, E. C.; Humbert, M. P.; Mellinger, Z. J.; Ren, Q.; Beebe, T. P.; Bao, L.; Chen, J. G. *J. Vac. Sci. Technol.* **2008**, *A26*, 23.
(24) Oyama, S. T. *The Chemistry of Transition Metal Carbides and Nitrides*; Blackie Academic and Professional: Glasgow, U.K., 1996.

a quartz-tube furnace and purged in nitrogen gas (50 sccm) for 20 min followed by a mixture of N_2, CH_4, and H_2 gases (5/30/5 sccm). Under this gas mixture, the temperature of the reactor bed was raised to 825 °C at a rate of 1 °C/min, held at 825 °C for 6 h, and then quenched to room temperature. Before exposure to air, all samples were passivated in a 1% O_2/N_2 gas mixture (50 sccm) at room temperature for a minimum of 1 h. 3DOM WO_3 material (0.1 g) was used for the indirect carburization procedure, whereas W-impregnated PMMA template (1.0 g) mixed with quartz sand (5 g) was used for the direct carburization. Both procedures resulted in approximately the same amount of 3DOM WC material (0.1−0.2 g).

2.3. Material Characterization. Scanning electron microscopy (SEM) images were obtained with a JSM-7400F (JEOL) microscope using an accelerating voltage of 3.0 kV. SEM samples were deposited onto a conductive carbon paper adhesive attached to a brass mount. Transmission electron microscopy (TEM) images were obtained using a JEM-2000FX (JEOL) microscope with LaB_6 filament and an accelerating voltage of 200 kV. TEM samples were prepared by sonicating small amounts of material in ethanol for several minutes. One or two drops of the suspension were transferred to a Lacey carbon support film deposited on a copper grid and allowed to dry for 24−48 h. Powder X-ray diffraction (XRD) patterns were recorded with a diffractometer (Rigaku, RINT UltimaIII) using CuKa radiation (tube voltage: 40 kV, tube current: 20 mA) equipped with a graphite monochromator. Crystallite sizes for WO_3(120) and WC(101) planes were calculated using the Scherrer equation from the width of peaks located at $2\theta = 26.6$ and 48.2°, respectively. Nitrogen adsorption measurements were performed using an Autosorb 6 (YUASA IONICS) sorption analyzer. Prior to the sorption measurements, 100−200 mg samples were degassed under a vacuum at 473 K for 1 h. Specific surface areas were calculated by the Brunauer−Emmet−Teller (BET) method. Thermogravimetric-differential thermal analysis (TG-DTA) measurements were performed with a TG-8120 (Rigaku) thermogravimetric analyzer. TGA samples (10 mg) were heated at a rate of 5, 10, or 15 °C/min to 800 °C under 25 sccm air flow or 2% O_2/N_2 gas mixture.

2.4. Methanol Electro-oxidation Using Cyclic Voltammetry (CV). The electrocatalytic activity of 3DOM WC and Pt-modified WC toward methanol oxidation was evaluated in methanol/sulfuric acid solution using cyclic voltammetry. A saturated calomel electrode (SCE, $E = +0.242$ V versus NHE) was used as the reference electrode for all experiments. WC material (5 mg) of was sonicated in ethanol/water solution (4 mL, v/v = 1/1) for 20 min. Nafion solution (5 wt %, 50 μL) was added to the mixture which was then further sonicated for another 20 min. The catalyst ink (20 μL) was placed on a 5 mm diameter glassy carbon electrode 5 μL at a time, with sufficient drying time between each transfer. The electrode was cleaned in 0.05 M H_2SO_4 solution performing 20 cycles with voltage sweep between −0.242 and 0.100 V vs SCE. Cyclic voltammetry experiments were performed in 0.5 M MeOH, 0.05 M H_2SO_4 aqueous solution with 500 cycles of linear sweeps between −0.242 and 1.008 V.

3. Results

3.1. Characterization. SEM images of 3DOM WC obtained from the indirect carburization of 3DOM WO_3 synthesized using the 490 and 180 nm PMMA template are displayed in images a and b in Figure 1, respectively. Ordered macroporous structure was obtained from the indirect carburization process for 490 and 370 nm templates at reasonable yields (~50%), whereas complete destruction of the structure was observed for the 260 and 180 nm templates. However, clear 3DOM structure at higher yield (> 80%) was observed upon the direct carburization of W-impregnated PMMA template with particle sizes ranging from 490 to 180 nm (Figure 1b and 1d). Furthermore, significant differences in the apparent surface structure of the materials resulting from direct and indirect carburization at much smaller length scales than the macroporous structure were observed (insets to images a and b in Figure 1). It should also be noted that a measurable decrease in pore size from the original PMMA template was observed for materials produced using both carburization procedures, typical of inverse opal synthesis. 3DOM WC produced using the 490 nm diameter PMMA template and indirect synthesis method displayed pore sizes of 428 ± 25 nm, whereas the direct synthesis method produced pore sizes of 371 ± 19 nm for the 490 nm PMMA and 149 ± 13 for the 180 nm PMMA.

TEM images of 3DOM WC samples obtained using 490 nm PMMA template and both carburization procedures demonstrated distinct differences (Figure 2). First, the WC crystallite size distributions varied significantly between the two synthesis methods. The indirect carburization resulted in large, smooth particles with occasionally dispersed agglomerations of smaller particles, whereas the direct carburization led to smaller particles with more serrated geometries and smaller size distribution. Second, a low-density film several nm thick was observed on the surface of the direct carburization material but not on that from indirect carburization (Figure 2, insets). The appearance of the film was attributed to residual amorphous carbon, possibly a result of incomplete decomposition of PMMA during carburization.

The XRD patterns for 3DOM WC samples synthesized using the indirect and direct carburization processes for varying mesopore-size are displayed in panels a and b in Figure 3, respectively. For indirect carburization, stoichiometric WC was obtained with almost no variation in the composition with varying macropore size. However, for direct carburization, small impurity peaks of W_2C and possibly WC_{1-x} appeared as the mesopore size was decreased. These impurities were likely a result of carbon-deficiency during the carburization process as partially decomposed PMMA or MMA monomer prevented methane gas from adsorbing and decomposing on the crystallite surface and entering the bulk phase. It is reasonable that the extent of impurities increased with decreasing pore size since mass transport through the 3DOM structure was reduced, therefore further inhibiting PMMA removal as well as CH_4 and H_2 adsorption/decomposition. Fortunately, the observed W_2C impurities were likely to reside at the core of the WC crystallites and should not affect the catalytic activity at the surface of the material. This notion of a carbon-deficient core was previously introduced by Giraudon et al. in their investigation of WO_3 carburization at various CH_4/H_2 partial pressures.[14]

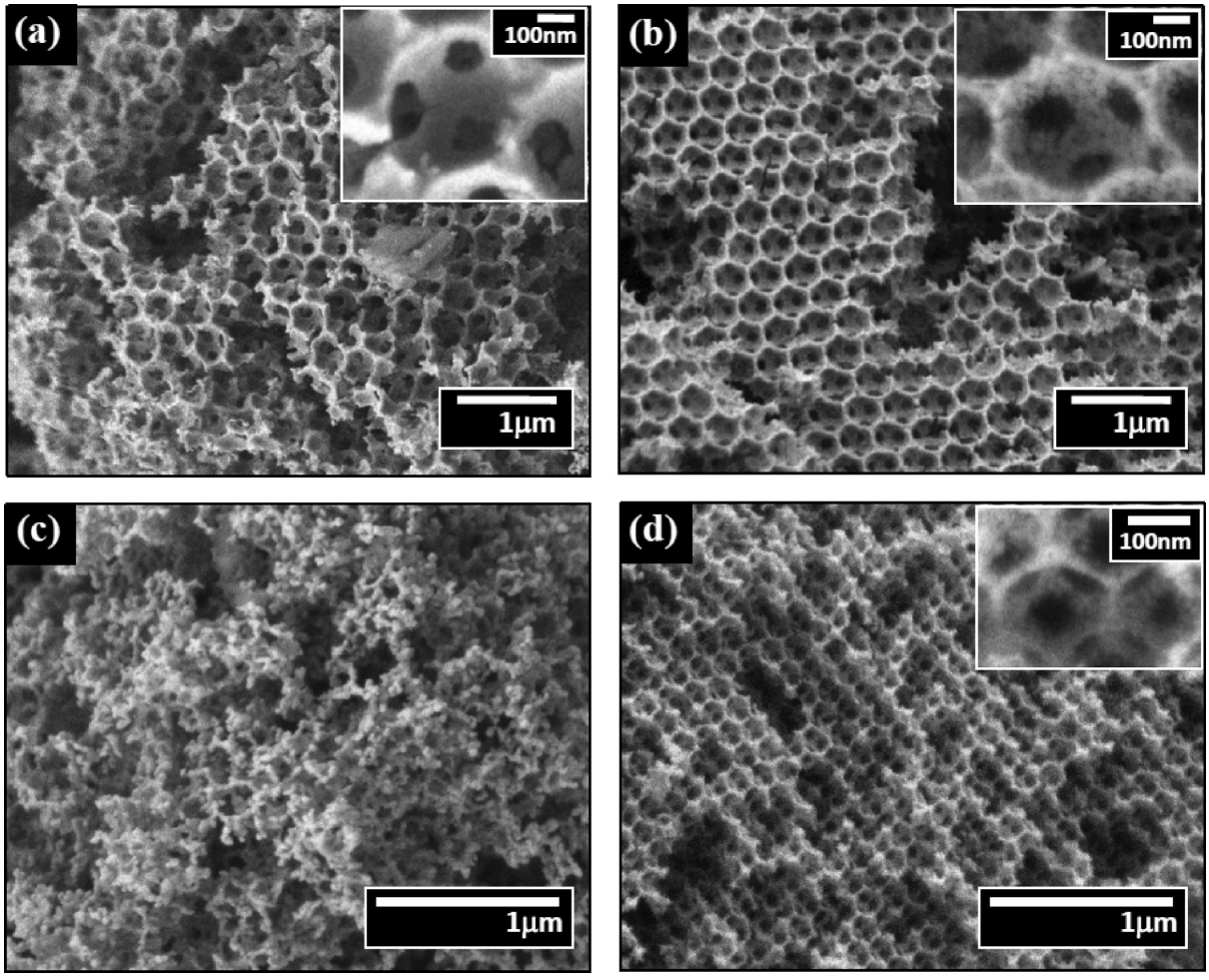

Figure 1. SEM images of WC structures obtained using (a) indirect and (b) direct carburization from PMMA template with 490 nm particle diameter and (c) indirect and (d) direct carburization from PMMA template with 180 nm diameter.

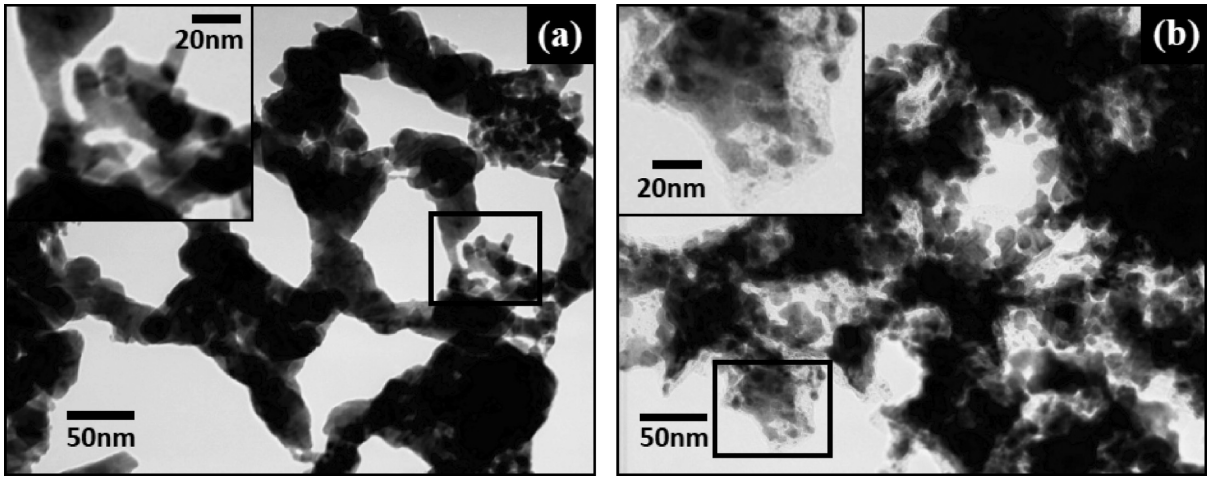

Figure 2. TEM images of 3DOM WC produced using (a) indirect carburization and (b) direct carburization procedures from 490 nm PMMA crystal template. Insets display magnification of the boxed regions within the images.

The XRD patterns for Pt-modified 3DOM WC samples showed a dramatic decrease in WC quality with increasing Pt metal loading (Figure 4). For both synthesis procedures, significant amounts of W_2C and WC_{1-x} impurities were observed. The 5 wt % Pt-metal loading resulted in a final bulk composition of W_2C, again independent of carburization procedure. The affinity for a carbon-deficient bulk composition appeared to be greater for the direct carburization method, with Pt-loading of 3 wt % also producing nearly pure W_2C, whereas WC peaks were still observed for the indirect method. It was not possible to observe the Pt XRD peaks for any of the WC samples. Approximate crystallite size of WO_3 or WC (when present) for 3DOM WO_3/WC, and

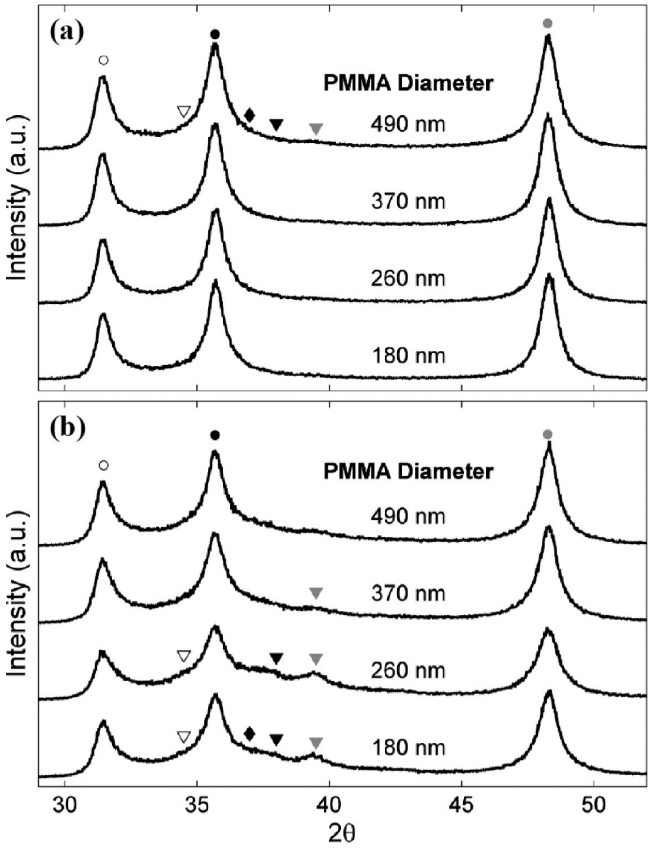

Figure 3. XRD spectra for 3DOM WC of varying PMMA template size produced using (a) indirect carburization and (b) direct carburization procedures. XRD peak labels are designated as follows: ○, WC(001), ●, WC(100), gray circle, WC(101) (PDF#051−0939); ▽, W_2C(100), ▼, W_2C(002), gray triangle, W_2C(101) (PDF#035−0776); and, WC_{1-x}(111) (PDF#020−1316).

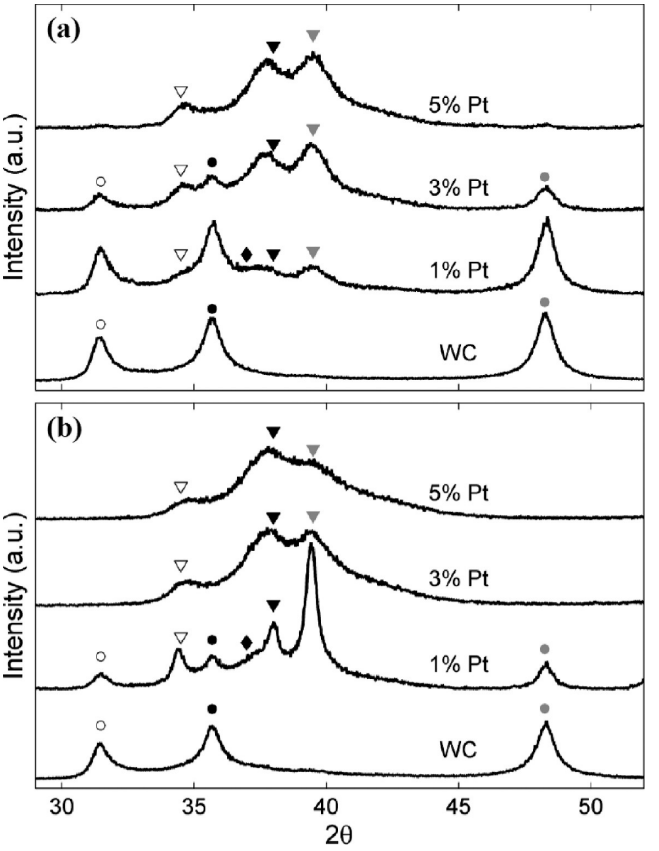

Figure 4. XRD spectra for Pt-modified 3DOM WC of varying Pt-loadings produced using (a) indirect carburization and (b) direct carburization procedures. XRD peak labels are designated as follows: ○, WC(001), ●, WC(100), gray circle, WC(101) (PDF#051−0939); ▽, W_2C(100), ▼, W_2C(002), gray triangle, W_2C(101) (PDF#035−0776); and, WC_{1-x}(111) (PDF#020−1316).

Pt-modified WO_3/WC materials were estimated using the Scherrer method and are summarized in Table 1.

Specific surface areas of the unmodified and Pt-modified 3DOM WO_3 and WC materials for both indirect and direct carburization procedures are displayed in Table 2. The BET results demonstrated a substantially higher surface area for 3DOM WC prepared using the direct method (40−56 $m^2\ g^{-1}$) compared to those using the indirect method (16−19 $m^2\ g^{-1}$) and 3DOM WO_3 (9−17 $m^2\ g^{-1}$) samples. The surface areas of the latter two materials agreed with calculated surface areas from crystallite sizes measured with XRD and assuming spherical particles of 17−19 $m^2\ g^{-1}$ and 9−12 $m^2\ g^{-1}$ for WC (indirect method) and WO_3, respectively. The WO_3 samples were observed to increase in surface area with decreasing pore size due to crystallite formation around the 3DOM skeleton as previously reported.[25] In contrast, 3DOM WC samples produced using the direct and indirect carburization methods had surface areas roughly independent of the observed pore size. Furthermore, Pt modification of WO_3 samples and WC made using the indirect method caused an increase in surface area with increasing Pt metal loading. However, surface areas of the direct carburization samples were found to be severely decreased upon Pt modification, although the surface area was again observed to increase with increasing metal loading.

Table 1. WO_3 and WC Crystallite Size Comparison of Direct and Indirect Synthesis Procedures As Determined from Scherrer Analysis of XRD Peaks

	crystallite diameter (nm)		
PMMA template sphere diameter	WO_3	WC (indirect)	WC (direct)
180 nm	36.8	11.1	9.6
260 nm	37.7	11.2	8.8
370 nm	39.2	10.8	10.1
490 nm	45.4	10.3	10.3
1 wt % Pt, 490 nm	41.4	10.8	13.4
3 wt % Pt, 490 nm	33.4	9.8	
5 wt % Pt, 490 nm	30.8		

Table 2. Specific Surface Areas of 3DOM WO_3, WC, and Pt-Modified WC As Determined by N_2 Adsorption and BET Analysis

	specific surface area ($m^2\ g^{-1}$)		
PMMA template sphere diameter	WO_3	WC (indirect)	WC (direct)
180 nm	17.1	16.0	54.2
260 nm	16.9	15.8	55.8
370 nm	13.4	17.8	41.0
490 nm	8.9	18.6	47.7
1 wt % Pt, 490 nm	10.4	24.1	28.7
3 wt % Pt, 490 nm	12.3	26.4	34.0
5 wt % Pt, 490 nm	13.6	28.2	38.0

Nitrogen adsorption isotherms were analyzed using BJH pore size distribution analysis. The 3DOM WC

(25) Sadakane, M.; Sasaki, K.; Kunioku, H.; Ohtani, B.; Ueda, W.; Abe, R. *Chem. Commun.* **2008**, 6552.

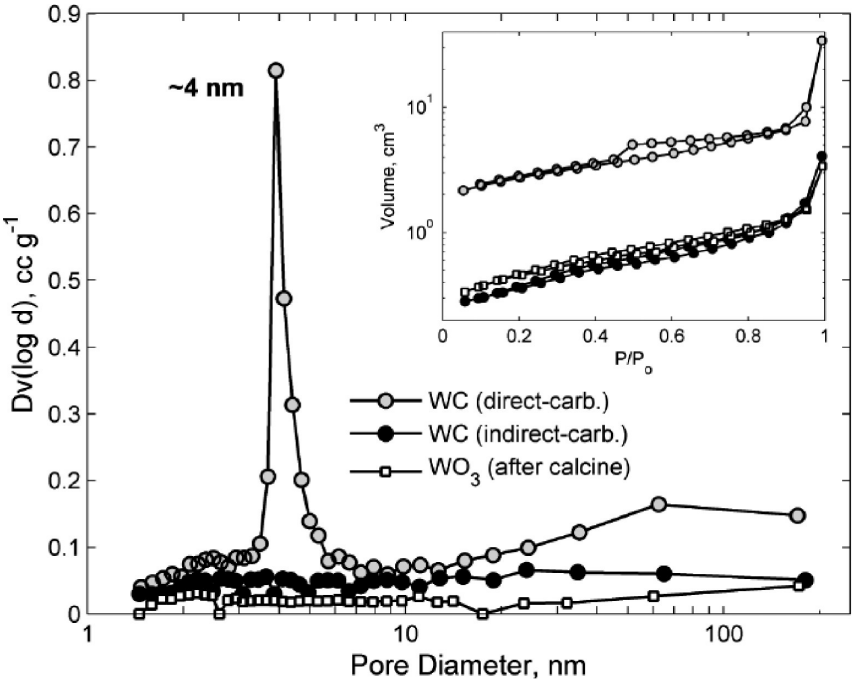

Figure 5. BJH pore-size distribution for 3DOM WO_3 and WC synthesized using both direct and indirect carburization methods with 490 nm PMMA template. Inlay displays corresponding N_2 adsorption/desorption isotherms used to calculate the pore-size distribution for all three materials.

material synthesized using the direct carburization procedure showed uniform mesoporosity, whereas the 3DOM WC produced using indirect carburization and 3DOM WO_3 samples demonstrated no porosity. A uniform pore size of approximately 4 nm was observed for the directly carburized 490 nm 3DOM sample (Figure 5). This feature was determined to be independent of the PMMA template size used during synthesis.

Thermogravimetric analysis was used to determine the percent excess carbon present in samples, assuming a WC bulk stoichiometry and complete oxidation of the sample to WO_3.[26] The excess carbon contents of samples created using direct carburization were found to have carbon impurities of 10.0, 11.2, 6.4, and 7.5 wt % for 3DOM WC samples synthesized using 180, 260, 370, and 490 nm PMMA templates, respectively. On the other hand, indirect carburization produced samples with carbon impurities of approximately 2 wt % or less, independent of the PMMA template size. The observed trend in specific surface area appears to increase linearly with carbon impurity (Figure 6).

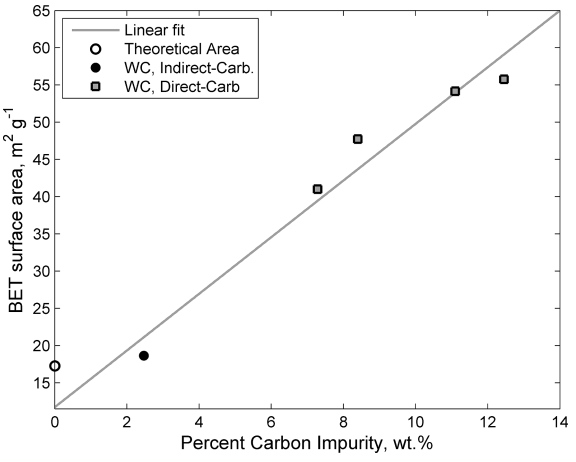

Figure 6. BET specific surface area ($m^2\ g^{-1}$) of 3DOM WC samples plotted versus carbon impurity (wt %) obtained using TGA demonstrating linear correlation between the two measurements. Theoretical data point for the surface area of WC sample with crystallite diameter of 10 nm calculated assuming perfectly spherical particles agglomerated within the 3DOM structure.

3.2. Electrochemical Oxidation of Methanol. The catalytic activities of 3DOM WC and Pt-modified 3DOM WC materials (synthesized from 490 nm PMMA template) toward methanol oxidation in 0.5 M MeOH and 0.05 M H_2SO_4 solution were evaluated using cyclic voltammetry (Figure 7). Relatively low activity toward MeOH electro-oxidation occurs on the unmodified WC produced using the indirect method, as indicated by a broad peak occurring between 0.4 and 0.6 V (Figure 7a). Substantial H_2 adsorption/desorption activity was also observed at approximately −0.05 and −0.1 V for positive and negative scans, respectively. In contrast, WC produced using the direct method demonstrated little or no activity for methanol electro-oxidation (Figure 7b), as well as a slightly lower hydrogen activity. The Pt-modified catalysts were observed to be far more active than the unmodified materials, with activity increasing with Pt loading (panels c and d in Figure 7).

A quantitative comparison of the catalytic activity was attempted by integration of the MeOH-oxidation peak in the potential range of 0.3 to 0.8 V using a polynomial

(26) The percent excess surface carbon was calculated assuming TGA samples of initial mass m_i, which contained both phase pure WC (m_{wc}) plus additional carbon mass (m_{xs}), were completely oxidized to a final mass of WO_3 (m_{wo_3}). Assuming all carbon was removed as CO_2 (with no other impurities present), the excess carbon mass was calculated as follows: $m_i = m_{wc} + m_{sx} = m_{wo_3}([MW\{WO_3\}]/[MW\{WC\}]) + m_{xs}$; $m_{xs} = m_i - m_{wo_3}([MW\{WO_3\}]/[MW\{WC\}])$; wt % excess carbon = m_{xs}/m_i.

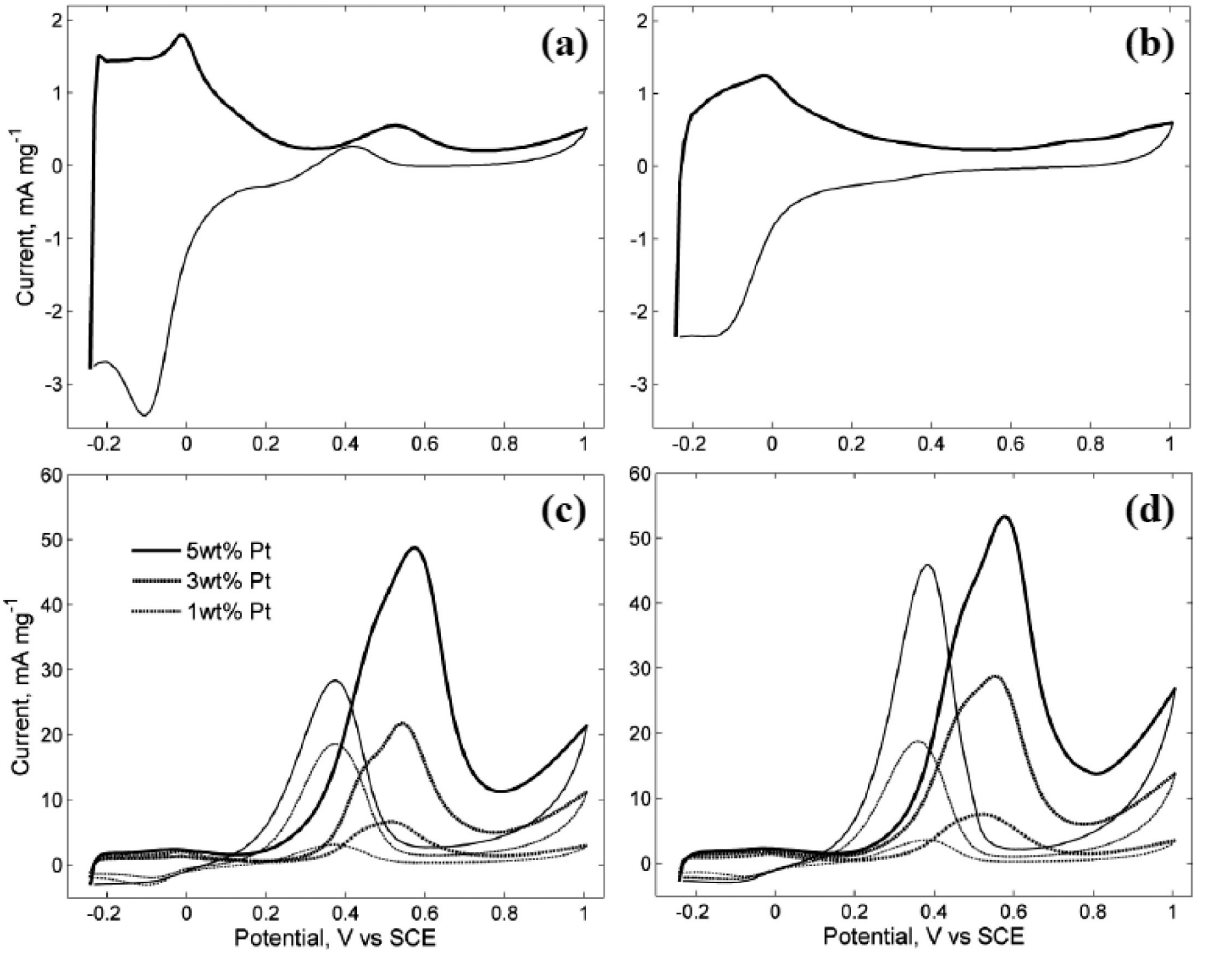

Figure 7. Comparison of methanol-oxidation over 3DOM WC and Pt-modified 3DOM WC produced using (a, c) indirect carburization and (b, d) direct carburization using cyclic voltammetry in 0.5 M MeOH and 0.05 M H_2SO_4 aqueous solution.

Table 3. Comparison of Methanol Oxidation Activities in Units of C $\mu g\{Pt\}^{-1}$ for Pt-Modified 3DOM WC Materials (Indirect and Direct Carburization) and Commercial 20 wt % Pt Supported on Carbon Black

	methanol oxidation activity (C $\mu g\{Pt\}^{-1}$)		
platinum loading	3DOM Pt-WC (indirect)	3DOM Pt-WC (direct)	commercial Pt/C
1 wt % Pt	2.69	3.38	
3 wt % Pt	2.86	4.22	
5 wt % Pt	4.28	**4.62**	
20 wt % Pt			2.39

baseline and normalized by the mass of Pt. Table 3 compares the resulting activities for Pt-modified 3DOM WC materials as well as a commercial 20 wt % Pt on carbon black (Alfa Aesar) in the unit of C $\mu g\{Pt\}^{-1}$. In summary, the Pt-modified 3DOM WC catalysts were found to be more active, per mass Pt, than the commercial catalyst in all cases. In addition, the direct carburization synthesis procedure resulted in a slightly more active catalyst than the indirect carburization procedure.

4. Discussion

From the experimental results, it was observed that there is an apparent trade-off between the quality of macroporous structure and material composition. Primarily, the indirect carburization procedure results in phase-pure WC with large crystallite size distribution and poor 3DOM structure, whereas direct carburization produces better structure with slightly carbon-deficient material. Furthermore, the addition of Pt metal severely reduces the WC composition, resulting in significant quantities of W_2C and WC_{1-x} phases, while having no observable effect on the macroporous structure.

All techniques used to characterize the 3DOM WC materials, particularly TEM, TGA, and N_2 adsorption experiments, point to the presence of an amorphous, mesoporous carbon film on the surface of samples produced using the direct carburization process. Materials produced using the indirect carburization method are void of the film, therefore exhibiting lower carbon impurities, lower specific surface areas, and no mesoporosity. The excess carbon observed in samples created using the direct method likely results from partially decomposed PMMA or MMA that is not removed during the carburization process. Ganeson et al. previously reported mesoporous features on tungsten carbide synthesized in the presence of polymer but attributed the mesoporosity to the tungsten carbide and not to excess surface carbon.[15] It is also observed that the carbon impurity increases as the sphere diameter of the PMMA template decreases. This relationship can be explained either by lower mass transport of reactant and product species during carburization or by a greater amount of PMMA

material in the bulk because of increased void fraction at smaller pore sizes.

The excess surface carbon is also likely responsible for increased retention of the 3DOM structure observed for the direct carburization material with smaller PMMA template. From TEM images, the amorphous carbon appears to completely cover the material surface, providing "cement" for holding the WC crystallites into the 3DOM structure. Without the carbon cement, the 3DOM structure does not survive carburization at smaller pore sizes, as demonstrated by samples made using the 260 and 180 nm PMMA templates and the indirect carburization method.

The amorphous carbon is observed to have a negative effect on the catalytic activity of the unmodified 3DOM WC toward methanol electro-oxidation. However, upon modification with Pt, samples produced using direct carburization demonstrate activities higher than those produced using the indirect procedure. One possible explanation for the enhanced activity could be that the carbon provides increased conductivity between WC crystallites, therefore increasing electrochemical activity. This effect is previously observed for hydrogen oxidation activity of mesoporous WO_3 impregnated with carbon black. The addition of carbon into the mesoporous structure was found to decrease the electrical resistance across samples, inversely proportional to the catalytic activity.[27]

5. Conclusions

The following conclusions regarding the synthesis and characterization of 3DOM WC materials can be drawn from our observations:

3DOM WC materials with pore size ranging from approximately 490 nm down to 180 nm were achievable using direct carburization of W-impregnated PMMA colloidal template. Indirect carburization resulted in destruction of the 3DOM structure for PMMA template diameters of 260 nm and smaller.

Indirect carburization of 3DOM WO_3 and direct carburization of W-impregnated PMMA template resulted in 3DOM WC materials with similar bulk compositions but dissimilar surface properties. The latter material contained mesoporous carbon, likely responsible for increased surface area measured by BET analysis and better retention of the 3DOM structure.

Modification of the W-impregnated PMMA template with Pt-metal prior to calcination/carburization resulted in significantly reduced phase purity of WC. Increased metal loading produced greater W_2C and WC_{1-x} impurities under identical synthesis conditions for both direct and indirect carburization procedures.

The unmodified 3DOM WC materials demonstrated low methanol electro-oxidation activity and significant hydrogen adsorption/desorption activity. Upon modification of 3DOM WC with Pt, substantial activity for methanol oxidation was observed, surpassing that of Pt supported on activated carbon on a per μg{Pt} basis.

Acknowledgment. The authors acknowledge support by the Department of Energy, Office of Basic Energy Sciences (Grant DE-FG02-00ER15104). J.P.B. also acknowledges partial support from the Goldwater Foundation.

(27) Cui, X.; Zhang, H.; Dong, X.; Chen, H.; Zhang, L.; Guo, L.; Shi, J. *J. Mater. Chem.* **2008**, *18*, 3575.